Aeroelastics Flight Dynamics Coupling Effects of the Semi Aeroelastic Hinge Device

A. Castrichini[1], T. Wilson[2]

Airbus Operations Ltd., Filton, BS99 7AR, United Kingdom

F. Saltari[3], F. Mastroddi[4], N. Viceconti[5]

La Sapienza University of Rome, 00184 Rome, Italy

J.E. Cooper[6]

University of Bristol, Bristol, BS8 1TH, United Kingdom

A recent consideration in aircraft design is the use of folding wing-tips with the aim of enabling higher aspect ratio aircraft with less induced drag, but also meeting airport gate limitations. This study investigates the impact of floating folding wing-tips on the aircraft flight dynamics. It is found that a floating wing-tips aircraft has similar handling qualities with respect to an aircraft with no wing extension.

Nomenclature

Symbols

b_j	=	Gust spanwise shape function
b_l	=	Aerodynamic lag-pole
c	=	Mean aerodynamic chord
$C_{()}$	=	Aerodynamic coefficient
D	=	Damping matrix
D_I	=	Inertial damping
e_1, e_2, e_3	=	PMA reference versors
H	=	Gust gradient
F_{Aero}	=	Aerodynamic forces vector
g	=	Gravity acceleration
T	=	Aerodynamic transformation matrix from inertial reference to PMA
u	=	Nodal displacement
u,v,w	=	Aircraft velocity components in the PMA
v_{cg}	=	Aircraft velocity in the PMA
V	=	Unperturbed air speed
w_j	=	Gust vector
w_g	=	Gust velocity
w_{g0}	=	Peak of the gust velocity
w_{ref}	=	Reference gust velocity
x_0	=	Gust origin position

[1] Loads and Aeroelastics Engineer

[2] Head of Technical Capability for Aircraft Loads Flight Physics

[3] Research Associate, Department of Mechanical and Aerospace Engineering

[4] Associate Professor, Department of Mechanical and Aerospace Engineering

[5] Master Student, Department of Mechanical and Aerospace Engineering

[6] Airbus Royal Academy of Engineering Sir George White Chair in Aerospace Engineering

J	=	Inertia tensor
k	=	Reduced frequency
K	=	Stiffness matrix
K_W	=	Inertial stiffness
K_θ	=	Torsional spring stiffness
L_g	=	Gust length
m	=	Aircraft mass
M	=	Mass matrix, Mach
M_{Hinge}	=	Hinge moment
q_f	=	Elastic modal displacement
q_{dyn}	=	Dynamic pressure
$Q_{()}$	=	Generalized aerodynamic force matrices
Q_e	=	External forces
$Q_{i()}$	=	Coefficient matrices of RFA
r_1	=	Aerodynamic states vector
S	=	Reference wing area
T_1	=	Transformation matrix from PMA to inertial reference
x_{cg}	=	Aircraft centre of mass position
x_j	=	j[th] panel's control node position
α	=	Angle of attack
γ_j	=	j[th] panel's dihedral angle
δ_{tj}	=	Kronecker delta
δ_x	=	Aerodynamic control surfaces vector
θ	=	Wing-tip folding angle
ξ	=	Generalised coordinate
Φ	=	Modal base
ψ	=	Vector of the Euler angles
ω	=	Angular velocity in the PMA
Superscript		
$\dot{}$	=	Differentiation with respect to time
$\sim$	=	Fourier transform
$\bar{}$	=	Generalized variable
$\hat{}$	=	Skew symmetric matrix
$'$	=	*V*ariable in the inertial reference system
Subscript		
e	=	Equilibrium value

I. Introduction

Much effort has been made to design aircraft to optimize fuel consumption through reduction of aerodynamic drag. A sizable contribution (30-40%) to the overall drag is lift-induced drag, which could be reduced by increasing the wing span, but such a design solution has well defined limits imposed by the maximum aircraft dimensions allowed at airports and also the increase in bending moments along the wing. A possible solution to the first issue is the use of folding wings that can be employed on the ground similar to the retractable wings used on aircraft-carrier-borne aircraft. The inclusion of such a design feature raises the question as to whether such a folding device could also be used to enable load reduction on the aircraft during the flight.

Recent works [1-5] have been aimed at studying the benefits of using a flexible wing-fold device for load alleviation and considering how it would be implemented on civil jet aircraft. The main idea consists of introducing a hinge in order to allow the wing tips to rotate, and it is known that the orientation of the hinge line relative to the airflow is a key parameter to enable successful load alleviation. When the hinge line is rotated outboard of the streamline, folding the wing-tip up introduces a decrease in the local angle-of-attack [1] and such an effect provides a means to reduce the loads acting on the wing, leading to the possibility of achieving a wing-tip extension with limited or even minimal impact on wing weight. Previous works have demonstrated that a free hinge is necessary in order to maximise the loads alleviation performance [1]. However, zero hinge stiffness leads the wingtip to be deflected during straight and level cruise flight due to the static trim loads, and furthermore, to a continuous oscillating motion due to unsteady aerodynamic loads. Such deflections and continuous motions are undesirable as they will be detrimental to the aerodynamic performance, and may lead to undesired rigid-body dynamic motion. Ideally, the wing-tip should not

deflect during cruise, but only operate once a significant gust is encountered. Such a concept is called Semi Aeroelastic Hinge (SAH). During the cruise, the wing-tip is kept in place by using a dedicated blocking mechanism. When a triggering event is detected, the wing-tip is actively released and the tip device acts then as a passive loads alleviation system, purely driven by the aerodynamic and inertial forces. After the loads event is finished, an actuator is then engaged to bring back the wing-tip to the initial clean configuration.

Previous works [1-5] focused on the impact of the SAH on the loads and flutter stability of a typical commercial jet aircraft. Now an investigation is made on the mutual influence between the aeroelastic effect of the wing-tip and the aircraft flight dynamics.

II. Aeroelastic Model

A. The Practical Mean Axis reference frame

Typical aeroelastic equations of motion (EOM) can be cast in the time domain as

$$\bar{M}\,\ddot{\xi} + \bar{D}\,\dot{\xi} + \bar{K}\,\xi = \bar{Q}_e + \bar{F}_{Aero}$$

$$\begin{bmatrix} mI & 0 & 0 \\ 0 & J & 0 \\ 0 & 0 & \bar{M}_{ff} \end{bmatrix} \begin{Bmatrix} \ddot{x}_{cg} \\ \ddot{\psi}_{cg} \\ \ddot{q}_f \end{Bmatrix} + \begin{bmatrix} 0 & 0 & 0 \\ 0 & 0 & 0 \\ 0 & 0 & \bar{D}_{ff} \end{bmatrix} \begin{Bmatrix} \dot{x}_{cg} \\ \dot{\psi}_{cg} \\ \dot{q}_f \end{Bmatrix} + \begin{bmatrix} 0 & 0 & 0 \\ 0 & 0 & 0 \\ 0 & 0 & \bar{K}_{ff} \end{bmatrix} \begin{Bmatrix} x_{cg} \\ \psi_{cg} \\ q_f \end{Bmatrix} = \begin{Bmatrix} \bar{Q}_{e_x} \\ \bar{Q}_{e_\psi} \\ \bar{Q}_{e_f} \end{Bmatrix} + \begin{Bmatrix} \bar{F}_{Aero_x} \\ \bar{F}_{Aero_\psi} \\ \bar{F}_{Aero_f} \end{Bmatrix} \quad (1)$$

where $\bar{M}$, $\bar{D}$, $\bar{K}$ are the generalised mass, damping and stiffness matrices, $\bar{Q}_e$ collects the non-aerodynamic external generalised forces (i.e. gravity), $\bar{F}_{Aero}$ are the generalised aeroelastic forces and ξ are the generalised displacements given by the aircraft centre of gravity position x_{cg}, the aircraft Euler angles ψ_{cg} and the elastic modal displacements q_f. These latter are related to a set of unconstrained mode shapes used to represent the linearized aircraft structural dynamics.

Several integrated models of flight dynamics and aeroelasticity have been proposed in the literature [6-11]. This work builds upon a simplified version of the formulation proposed by Saltari el al. [6]. The rigid body degrees of freedom are here associated with a set of practical mean axes (PMAs). Such a reference has its origin at the instantaneous aircraft centre of mass, but the orientation is fixed to the mean axes at the undeformed configuration.

The rigid body modes have to represent unitary translations x_{cg} and rotations ψ_{cg} around the aircraft centre of mass at the undeformed configuration. The set of eigenvectors Φ is taken consistent with the velocities and angular velocities defined positive in flight dynamics (*e.g.* a positive forward speed) allowing a better comprehension of the results concerning the rigid-body variables.

The structural physical displacements u expressed on a modal basis as

$$u(x,t) = \sum_{n=1}^{N_{Modes}} \Phi(x)\,\xi(t) \tag{2}$$

this kind of formulation introduces a significant approximation since only a limited number of structural modes are used. Only a number of modes equal to the structural degrees of freedom prevents any loss in accuracy in the passage from the physical displacement base to a modal base.

B. Inertial Modelling

Inertial coupling effects are generally considered of secondary importance [6] compared to the effects provided by the aerodynamics and have been here partially neglected. However, in general formulation of integrated flight dynamics and aeroelasticity, one may consider the rigid-body equations of motion expressed with respect to a non-inertial frame of reference. In aeroelastic framework, the rigid-body motion is expressed with respect to the FEM frame, moving in a uniform rectilinear motion with respect to the inertial frame. Thus, some further inertial and weight projection effects arise. More specifically, the absolute acceleration and angular momentum can be expressed with respect to the non-inertial frame of reference attached to the PMAs:

$$\begin{aligned} \frac{D\boldsymbol{v_{cg}}}{Dt} &= \dot{\boldsymbol{v}}_{\boldsymbol{cg}} + \boldsymbol{\omega} \times \boldsymbol{v_{cg}} \simeq \Delta\dot{\boldsymbol{v}}_{\boldsymbol{cg}} - \boldsymbol{v_{cg_e}} \times \Delta\boldsymbol{\omega} \\ \frac{D(\boldsymbol{J\omega})}{Dt} &= \boldsymbol{J}\dot{\boldsymbol{\omega}} + \boldsymbol{\omega} \times \boldsymbol{J\omega} \simeq \boldsymbol{J}\Delta\dot{\boldsymbol{\omega}} \end{aligned} \tag{3}$$

where $\boldsymbol{v_{cg}}$ and $\boldsymbol{\omega}$ are the velocity and angular velocity physical entities, whereas $\boldsymbol{J}$ is the inertia tensor.

For a linearized analysis, the components of angular velocity $\boldsymbol{\omega}$ coincide with the derivative of Euler angles $\Delta\psi$. On the other hand, the component of $\boldsymbol{v}_{cg}$ will be expressed in the non-inertial frame of reference and denoted as v_{cg}. The position of the body in the inertial frame of reference can thus be recast as

$$\begin{gathered} \Delta\dot{x}_{cg} = \Delta v_{cg} - \hat{v}_{cg_e}\,\Delta\psi \\ \dot{\xi}' = T_1\,\dot{\xi} \end{gathered} \tag{4}$$

where

$$T_1 = \begin{bmatrix} I & -\hat{v}_{cg_e} & 0 \\ 0 & I & 0 \\ 0 & 0 & I \end{bmatrix}$$

Summarizing the concepts above, the EOM will be recast with respect to ξ and ξ' defined as

$$\xi' = \begin{Bmatrix} \Delta x_{cg} \\ \Delta\psi \\ \Delta q_f \end{Bmatrix};\ \dot{\xi} = \begin{Bmatrix} \Delta v_{cg} \\ \Delta\omega \\ \Delta\dot{q}_f \end{Bmatrix};$$

Skipping the intermediate passages for the sake of conciseness, the following damping matrix D_I allows to switch the EOM from the inertial to non-inertial frame in case of small perturbations around a steady rectilinear flight

$$\overline{D}_I = \begin{bmatrix} 0 & -m\hat{v}_{cg_e} & 0 \\ 0 & 0 & 0 \\ 0 & 0 & 0 \end{bmatrix} \tag{5}$$

where V is the trim speed.

Moreover, the description of the aircraft motion in the PMA non-inertial reference requires accounting for the projection of the weight force on the aircraft body reference. Under the assumption of small perturbation with respect to the trimmed configuration, such a contribution was modelled as an additional stiffness term, to be added to $\overline{K}$, and defined as

$$\bar{K}_W = mg\begin{bmatrix} 0 & 0 & 0 & 0 & 1 & 0 & & \\ 0 & 0 & 0 & 1 & 0 & 0 & \cdots & 0 \\ 0 & 0 & 0 & 0 & 0 & 0 & & \\ & \vdots & & & \vdots & & \ddots & \vdots \\ & 0 & & & 0 & & \cdots & 0 \end{bmatrix} = \begin{bmatrix} 0 & m\hat{g} & 0 \\ 0 & 0 & 0 \\ 0 & 0 & 0 \end{bmatrix} \tag{6}$$

with mg the weight of the aircraft.

C. Aerodynamic Modelling

Unsteady aerodynamic effects are modelled using the Doublet Lattice Method [12, 13] (DLM). The same modal formulation employed to model the structural dynamics, is used to describe the unsteady aerodynamic forces which are therefore strongly dependent on the number of modes used. In the frequency domain, DLM unsteady aerodynamic forces are defined, as [13]

$$\tilde{F}'_{Aero} = q_{dyn}[Q'_{hh}(M,k)\tilde{\xi}'_h + Q'_{hx}(M)\tilde{\delta}_x + Q'_{hj}(M,k)\tilde{w}_j] \tag{7}$$

where Q'_{hh} ($\mathrm{N_{Modes}}$ x $\mathrm{N_{Modes}}$), Q'_{hx} ($\mathrm{N_{Modes}}$ x $\mathrm{N_{ControlSurf}}$), Q'_{hj} ($\mathrm{N_{Modes}}$ x $\mathrm{N_{Panels}}$), are respectively the generalized aerodynamic forces matrices related to the Fourier Transform of the generalized coordinates $\tilde{\xi}_h$, control surfaces vector $\tilde{\delta}_x$ and gust shape $\tilde{w}_j$ and q_{dyn} $\left(q_{dyn} = \frac{1}{2}\rho V^2\right)$ is the dynamic pressure.

The gust vector defines the downwash on a generic aerodynamic panel j due to the gust such that

$$w_j = b_j(y)\cos\gamma_j \frac{w_{g0}}{2V}\left(1 - cos\left(\frac{2\pi V}{L_g}\left(t - \frac{x_0 - x_j}{V}\right)\right)\right)\delta_{t_j} \tag{8}$$

where, L_g is the gust length (twice the gust gradient H), δ_{t_j} is a Kronecker Delta which is equal to 1 only in the time window when the gust crosses the j^{th} panel $\left(\frac{x_0 - x_j}{V} \le t_j \le \frac{x_0 - x_j}{V} + \frac{V}{L_g}\right)$, b_j is a shape function defining the gust spanwise shape and w_{g0} the peak gust velocity, the latter defined (in m/s) as [14]

$$w_{g0} = w_{ref}\left(\frac{H}{106.17}\right)^{\frac{1}{6}} \tag{9}$$

For computational efficiency the AIC, and therefore the GAF, matrices are generated for a limited set of reduced frequencies $\left(k = \frac{\omega c}{2V}\right)$ and Mach numbers; the remaining intermediate values are evaluated through interpolation schemes [13].

As for the mass, damping and stiffness, also the aerodynamic matrices are expressed in the PMA reference system. The DLM GAF matrices are formulated in the inertial reference system [12, 13] under the assumption of steady longitudinal flight. As result of such a formulation, any variation of pitch angle or yaw are considered as equivalent variations of aerodynamic angle of attack and sideslip respectively. In the PMA reference formulation instead, a static rotation of an aircraft does not generate any aerodynamic forces perturbation. Such a correction, on the rigid body aerodynamic forces, is achieved by post multiplying the Q'_{hh} matrix, expressed in the inertial frame of reference, with a transformation matrix T ($\mathrm{N_{Modes}}$ x $\mathrm{N_{Modes}}$) [6] such that

$$Q_{hh}(k, M) = Q'_{hh}(k, M)T(k) \tag{10}$$

where

$$T(k) = \begin{bmatrix} 1 & 0 & 0 & 0 & 0 & 0 & & \\ 0 & 1 & 0 & 0 & 0 & b/jk & & \\ 0 & 0 & 1 & 0 & b/jk & 0 & \cdots & 0 \\ 0 & 0 & 0 & 1 & 0 & 0 & & \\ 0 & 0 & 0 & 0 & 1 & 0 & & \\ 0 & 0 & 0 & 0 & 0 & 1 & & \\ & & & \vdots & & & \ddots & \vdots \\ & & & 0 & & & \cdots & 1 \end{bmatrix}$$

where the elastic modes related block is set equal to the identity matrix, since the definition of the elastic modes of the system is kept unchanged.

The aerodynamic forces are then recast in a time domain formulation using the Rational Fraction Approximation (RFA) method proposed by Roger [15] such that

$$F_{Aero} = q_{dyn}\left\{\left[Q_{hh0}\xi_h + \frac{c}{2V}Q_{hh1}\dot{\xi}_h + \left(\frac{c}{2V}\right)^2 Q_{hh2}\ddot{\xi}_h\right] + [Q_{hx0}\delta_x]\right.$$
$$\left. + \left[Q_{hj0}w_j + \frac{c}{2V}Q_{hj1}\dot{w}_j + \left(\frac{c}{2V}\right)^2 Q_{hj2}\ddot{w}_j\right] + \sum_{l=1}^{N_{Poles}} r_l\right\} \tag{11}$$

where r_l is the generic aerodynamic state vector related to the generic lag-pole $b_l = \frac{k_{max}}{l}$. These extra states allow the modelling of the unsteady response of the aerodynamics by taking into account of the delay of the aerodynamic forces with respect to the structural deformations. These aerodynamic states were evaluated through the set of dynamic equations

$$\dot{r}_l = -b_l\frac{2V}{c}Ir_l + Q'_{hh2+l}\dot{\xi}'_h + Q'_{hj2+l}\dot{w}_j \qquad l = 1, \dots, N_{Poles} \tag{12}$$

which are solved together with the equations of motion (1).

The matrices Q_{hh0}, Q_{hh1} and Q_{hh2} have the physical meaning of aerodynamic stiffness, damping and inertia respectively. The transformation introduced in Eq. (10) led to have the first six columns of Q_{hh0} equal to zero, meaning that no aerodynamic stiffness is associated with the rigid body modes.

Further aerodynamic correction terms are also introduced to account for aerodynamic contribution that are in general neglected by the DLM such as the aerodynamic drag. This latter contribution can be expressed as

$$D = q_{dyn}C_D = q_{dyn}S\left(C_{D_0} + C_{D_\alpha}\alpha\right) \tag{13}$$

The perturbation of the aerodynamic drag from the equilibrium value, due to a variation of longitudinal velocity and angle of attack can be obtained by linearising Eq.(13) as

$$\left.\frac{\partial D}{\partial u}\right|_{D_e} = \rho V S C_{D_e} = \frac{2q_{dyn}S}{V^2}C_{D_e} \tag{14}$$

$$\left.\frac{\partial D}{\partial \alpha}\right|_{D_e} = \left.\frac{\partial D}{\partial w}\right|_{D_e} = q_{dyn} S C_{D_\alpha} = \frac{q_{dyn} S}{V} C_{D_\alpha}$$

and these terms represent the additional aerodynamic damping contributions that affect the longitudinal aircraft dynamics and can be collected in the damping matrix $Q_{hh1D}(\mathrm{N_{Modes}\ x\ N_{Modes}})$ [6] defined as

$$Q_{hh1D} = \begin{bmatrix} -2C_{D_e}S/c & 0 & -C_{D_\alpha}S/c & 0 & 0 & 0 & & \\ 0 & 0 & 0 & 0 & 0 & 0 & & \\ 0 & 0 & 0 & 0 & 0 & 0 & \cdots & 0 \\ 0 & 0 & 0 & 0 & 0 & 0 & & \\ 0 & 0 & 0 & 0 & 0 & 0 & & \\ 0 & 0 & 0 & 0 & 0 & 0 & & \\ & & \vdots & & & & \ddots & \vdots \\ & & 0 & & & & \cdots & 0 \end{bmatrix} \tag{15}$$

The DLM GAF matrices are evaluated at zero angle of attack, however the EOM are linearized around a trimmed configuration, hence the aerodynamics loads acting on an unconstrained aircraft should be corrected in order to account for the effects of a non-zero angle of attack. These quasi-steady effects are particularly relevant in flight dynamics in terms of rigid body response and stability, and are due to the aerodynamic forces introduced by a perturbation of dynamic pressure and angle of attack being a function of the equilibrium angle of attack. These contributions can be modelled by assuming that a perturbation of dynamic pressure results in a variation of the local lift magnitude, whereas a perturbation of the angle of attack reflects in a variation of the local lift direction. Both these terms are evaluated by linearizing the trim aerodynamic forces distribution with respect to the longitudinal speed and angle of attack as

$$\Delta F_{Aero} = -2\frac{F_{AeroTrim}}{V}\Delta u + F_{AeroTrim} \cdot e_3 \frac{\Delta w}{V} e_1 \tag{16}$$

Such a linearization results in the definition of to further matrices $Q'_{hh1\alpha}$ and $Q'_{hh1q_{dyn}}$ to be added to the aerodynamic stiffness matrix Q'_{hh1}. Saltari et al. [6] provide further details on the derivation of these terms.

D. Final Formulation of Equation of Motion

A nonlinear reduced order model is defined to model the linear and nonlinear hinge mechanisms. The idea is to use the set of flexible modes obtained when a very low hinge spring stiffness is defined along the hinge line; a zero stiffness value was avoided to prevent numerical singularities during the modal analysis. This approach showed the first two flexible modes to be local symmetric and anti-symmetric pseudo-rigid wing-tips deflection as shown in Fig. 1(a, b). Such modal shapes are by definition orthogonal with the remaining flexible modes that involve a combination of wing-tips and main airframe deformations, Fig. 1(c, d), therefore they could be used to describe independent wing-tip rotations. The overall span reduction due to the wing-tips deflection was not considered.

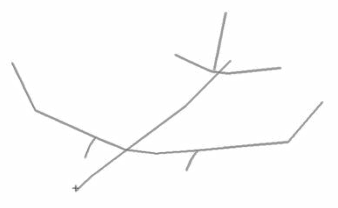

(a) 7st Mode *4.17E-3 Hz*

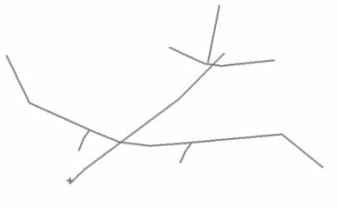

(b) 8nd Mode *4.18E-3 Hz*

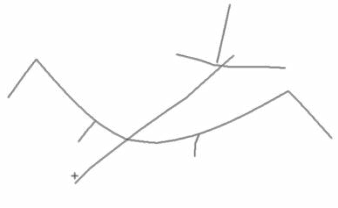

(c) 9rd Mode *2.22E0 Hz*

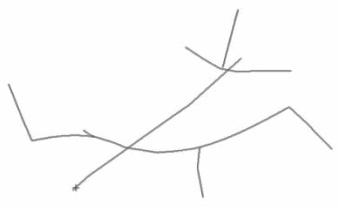

(b) 10th Mode *2.54E0 Hz*

Figure 1. Typical Flexible Modes of an Aircraft with the Folding Wing-Tips

Linear and nonlinear hinge devices, such as springs, dampers or actuators, can be modelled by applying external moments on the hinge nodes along the hinge axis in order to simulate the related restoring moments on the wing-tips and main airframe, as shown in Fig. 2. The hinge moments could be defined as linear or nonlinear functions of the wing-tip folding angle and, once projected onto the structural modes, defined as a set of generalized forces that could excite mainly the local wing-tip modes and so drive the wing-tips motion.

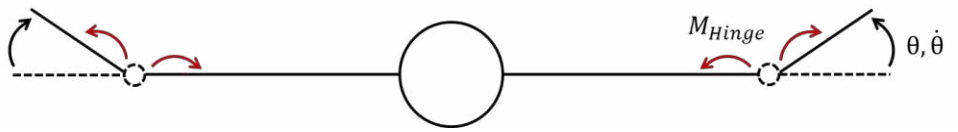

Figure 2. Applied Hinge Moments

The aerodynamic forces are given by

$$F_{AeroTot} = q_{dyn}\left\{\left[Q_{hh0}\xi'_h + \frac{c}{2V}\left(Q_{hh1} + Q_{hh1D} + Q_{hh1\alpha} + Q_{hh1q_{dyn}}\right)\dot{\xi}_h + \left(\frac{c}{2V}\right)^2 Q_{hh2}\ddot{\xi}_h\right]\right.$$
$$\left. + \left[Q_{hx0}\delta_x\right] + \left[Q_{hj0}w_j + \frac{c}{2V}Q_{hj1}\dot{w}_j + \left(\frac{c}{2V}\right)^2 Q_{hj2}\ddot{w}_j\right] + \sum_{l=1}^{N_{Poles}} r_l\right\} \tag{18}$$

and final stiffness and damping matrices are expressed as

$$\overline{K}_{Tot} = \overline{K} + \overline{K}_W \tag{19}$$

$$D_{Tot} = \overline{D} + \overline{D}_I \tag{20}$$

The linear and nonlinear hinge mechanisms are simulated through the introduction of the generalised nonlinear force M'_{Hinge}. The idea is to simulate a mechanism that allows the wing-tip to rotate only when the aerodynamic forces are higher than some predefined threshold value. Such a device was modelled by applying, to the wing-tips and main airframe, the restoring moments due to a piecewise linear spring whose stiffness was varied according to the loads experienced by the aircraft such that

$$M_{Hinge} = -K_\theta\theta$$
$$\begin{cases} K_\theta = 1.E^{12}Nm/rad & if \quad 0 < t < t_{release} \\ K_\theta = 1.E^{0}Nm/rad & if \quad t \geq t_{release} \end{cases} \tag{21}$$

III. Numerical Results

A single aisle aircraft linear structural model is used for the analyses. The wing-tip extensions are connected to the main wing structure in a similar way as in previous work [1]. The total span is increased by roughly 25%. A single flight point was considered at 25000 ft of altitude and a Mach number of M=0.82.

A series of dynamic and static analyses have been performed in order to asses the open-loop response of an aircraft with free and fixed wing-tips with respect to a baseline model without the tip extension. The three models have the same control surfaces. The three models share the same mass distribution for the fuselage, engines, tail planes and inner wing. The same mass was assumed for the hinge mechanism and wing-tips of free and fixed hinge models to account for the fact that a wing span extension would require in any case a hinge mechanism to allow the wing folding whilst on the ground.

A. Aerodynamic derivatives and handling qualities

This section presents an investigation of the impact of the SAH on the aircraft aerodynamic derivatives and handling qualities. Figure 3 reports the variation of some aerodynamic derivatives for different dynamic pressure values. The aircraft with the free folding wing-tip shows very close aerodynamic derivatives with respect to the baseline model. In terms of CL_α this is easily justifiable by the fact that an increment of the angle of attack generates an upward deflection of the wingtip resulting in negative incremental aerodynamic loads thus reducing the CL_α to the same level of the baseline aircraft with a smaller wing. The same comments are valid for Cm_α which decreases passing from a fixed to a free hinge.

A significant impact is observed in terms of rolling damping Cl_p between free and fixed wing-tip configurations. A well know problem associated to high aspect ratio wing, is the reduction of rolling authority due to the increment of rolling damping introduced by the longer span. Having free wing-tips seems to overcome this limitation leading to comparable roll damping levels of an aircraft without the wing extension. Such an improvement of the rolling handling qualities can be explained by analysing the aerodynamic forces generated during the manoeuvre. In the case of a positive roll manoeuvre, the right wing tends to go down whereas the left wing goes up. The incremental aerodynamic forces induced by the roll rate will generate an incremental upward deflection of the right wing-tip while the left wing-tip will see a reduction of the folding angle. The resulting rolling moment induced by the aeroelastic loads will have

the same sense of the rolling moment induced by the aileron, as shown in Fig. 4. Moreover, the variation of angle of attack introduced by the wing-tip deflection, is constant all over the tip surface whereas the roll rate generates higher variation of the local angle of attack toward the tip. As results the wing tip deflection will generate an incremental lift contribution which is closer to the hinge with respect to the incremental lift induced by the roll rate. Since a perfect free hinge cannot pass any bending moment, such a condition is satisfied (neglecting the inertial terms) only if the local lift contribution due to the wing-tip deflection is higher than the one due to the roll rate. As a consequence the hinges see net shear forces which aid the rolling manoeuvre thus increasing the rolling authority of the aileron.

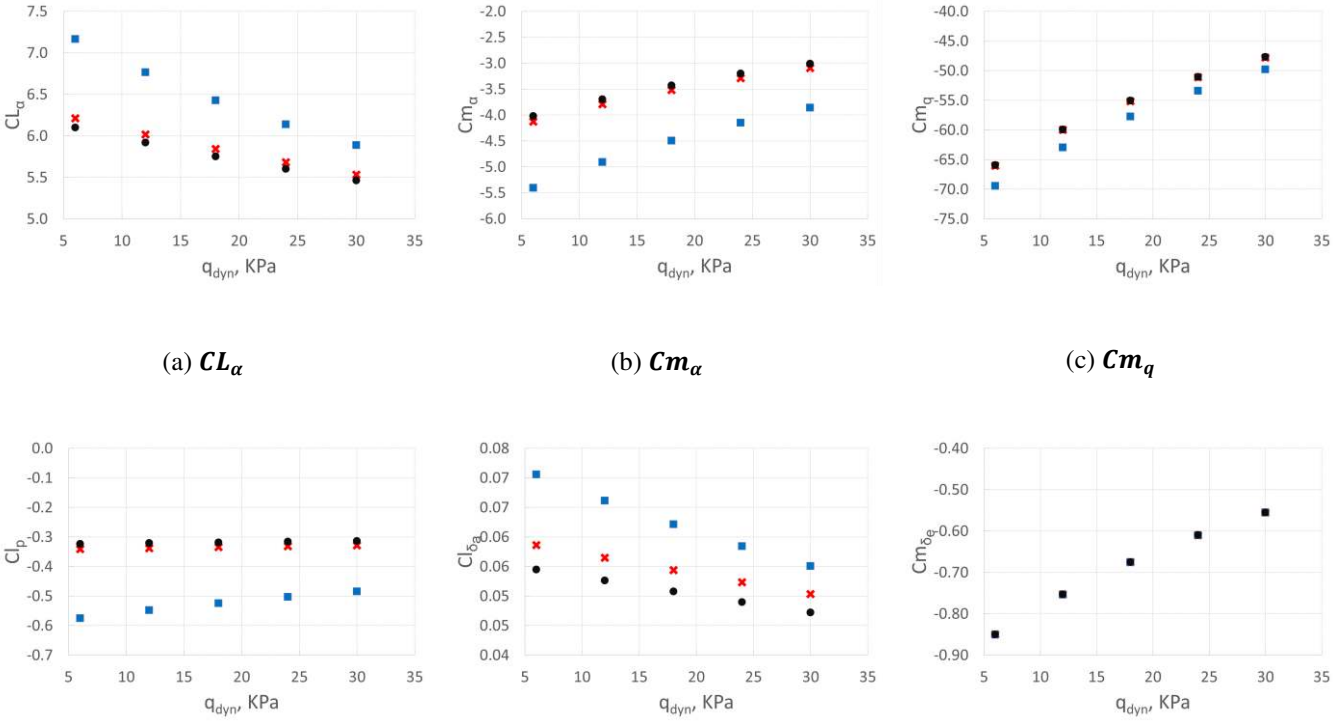

(a) $\boldsymbol{CL_\alpha}$ (b) $\boldsymbol{Cm_\alpha}$ (c) $\boldsymbol{Cm_q}$

(d) $\boldsymbol{Cl_p}$ (e) $\boldsymbol{Cl_{\delta_a}}$ (f) $\boldsymbol{Cm_{\delta_e}}$

Figure 3. Aerodynamic Derivative

(black dot: baseline; blue square: fixed hinge; red cross: free hinge)

Figure 3(e) shows the rolling moment coefficient introduced by the aileron. Despite the three models sharing the

same aileron, different values are observed between the baseline, the free and the fixed hinge aircraft even for low dynamic pressure where the aeroelastic effects are less pronounced. This finding is due to the fact that the aileron is placed close to the hinge, as a consequence, for a longer span aircraft, an aileron deflection will produce spill over aerodynamic forces that will interest also part of the tip, as shown in Fig. 4(a). This would lead the local aileron centre of pressure to move outboard thus increasing the moment arm. Moreover Fig. 3(e) shows also that the rolling moment coefficient of the free wing-tip aircraft has a lower gradient with respect to the fixed hinge one leading to a delay of the aileron reversal when the floating tips are employed. Such an effect is due to the fact that the aerodynamic forces produced by the tips deflection tend to reduce the wing bending, this reflects in a reduction of the wing torsion, in the case of a sweepback wing, and thus on a positive impact on the aileron reversal.

A small impact is observed also for Cm_q, whereas Cm_{δ_e} does not vary between the three aircraft.

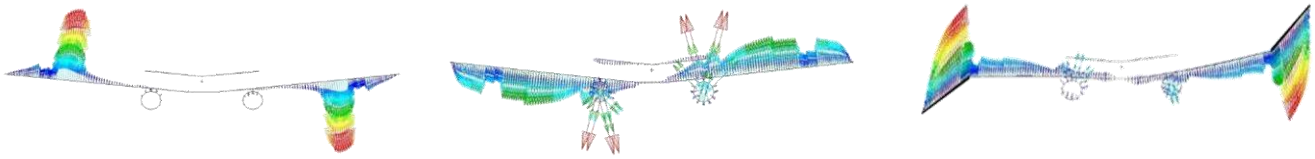

(a) Aileron aerodynamic forces (b) Roll rate aerodynamic forces (c) Aeroelastic aerodynamic forces

Figure 4. Aerodynamic Forces Contributions Due to a Rolling Manoeuvre

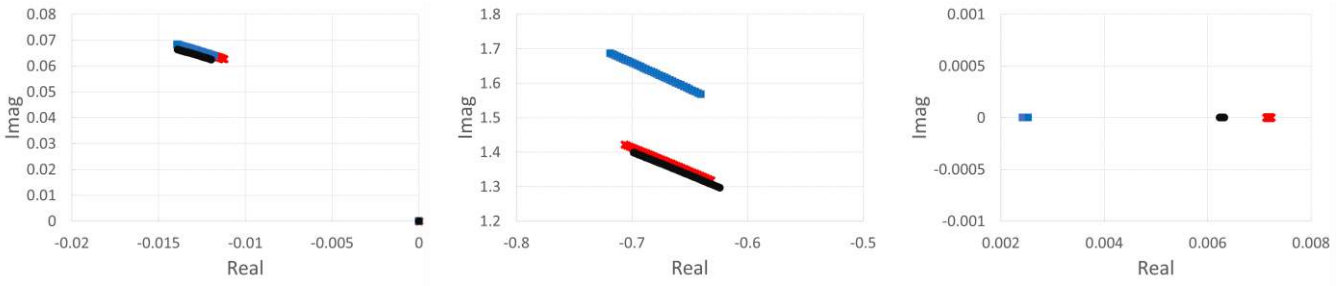

(a) Phugoid (b) Short Period (c) Spiral

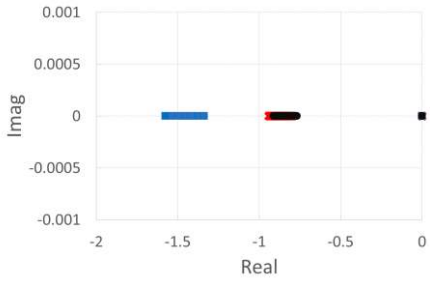

(d) Roll

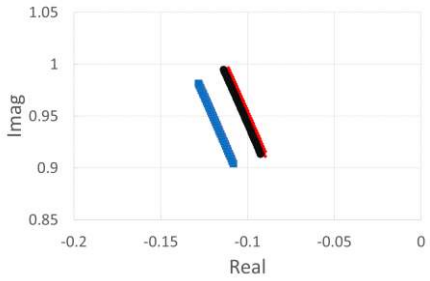

(e) Dutch Roll

Figure 5. Root Locus

(black dot: baseline; blue square: fixed hinge; red cross: free hinge)

Figure 5 reports the evolution of root locus of the aeroelastic system for different values of dynamic pressure, particular attention is given to the flight dynamics modes. No significant impact is observed for the long period mode. As regards the short period motion, a variation is observed between the fixed and the free hinge aircraft, with the latter having almost the same values of the baseline condition. The three aircraft share similar values for the real part of the poles, but with the fixed hinge aircraft showing higher imaginary values. This finding would indicates the three models to have similarly damped short period modes, but with higher frequency for the fixed hinge case. The spiral mode is unstable for all the analysed configurations and the use of a free hinge seems to destabilise even further such a dynamics. This is usually not a problem since many aircraft have an unstable spiral model which can be easily stabilised with a proper control law. As regard the roll and dutch roll, almost no impact on the frequency and a reduction of the damping is observed between the fixed and the free hinge aircraft in agreement with what was shown in Fig 4(d). Again, the free hinge shows values that are similar to the baseline ones.

B. Dynamic manoeuvres

In this section, a comparison is made between the free, fixed hinge and baseline model response to a time varying command on the aileron, elevator and rudder respectively.

Figure 6 shows the aircraft response to an aileron command. The command time history is shown in Fig. 6(f). The plots shows that the free hinge aircraft has the same dynamic response of the baseline model achieving a higher roll

rate with respect to the fix hinge aircraft. This is in agreement with what has been shown in the previous section. Figure 6(e) reports the asymmetric wing-tip deflection induced by the manoeuvre.

Figure 7 reports the dynamic response due to an elevator deflection. Again, the free hinge aircraft shows the same response as the baseline. Lower pitch and altitude variation are observed for the fixed hinge aircraft.

As regards the response due to the rudder, shown in Fig. 8, the free hinge and the baseline model report higher roll rate, but slower yaw rate, when compared to the fixed hinge aircraft. Also, in this case, an asymmetric deflection of the wing-tips is observed.

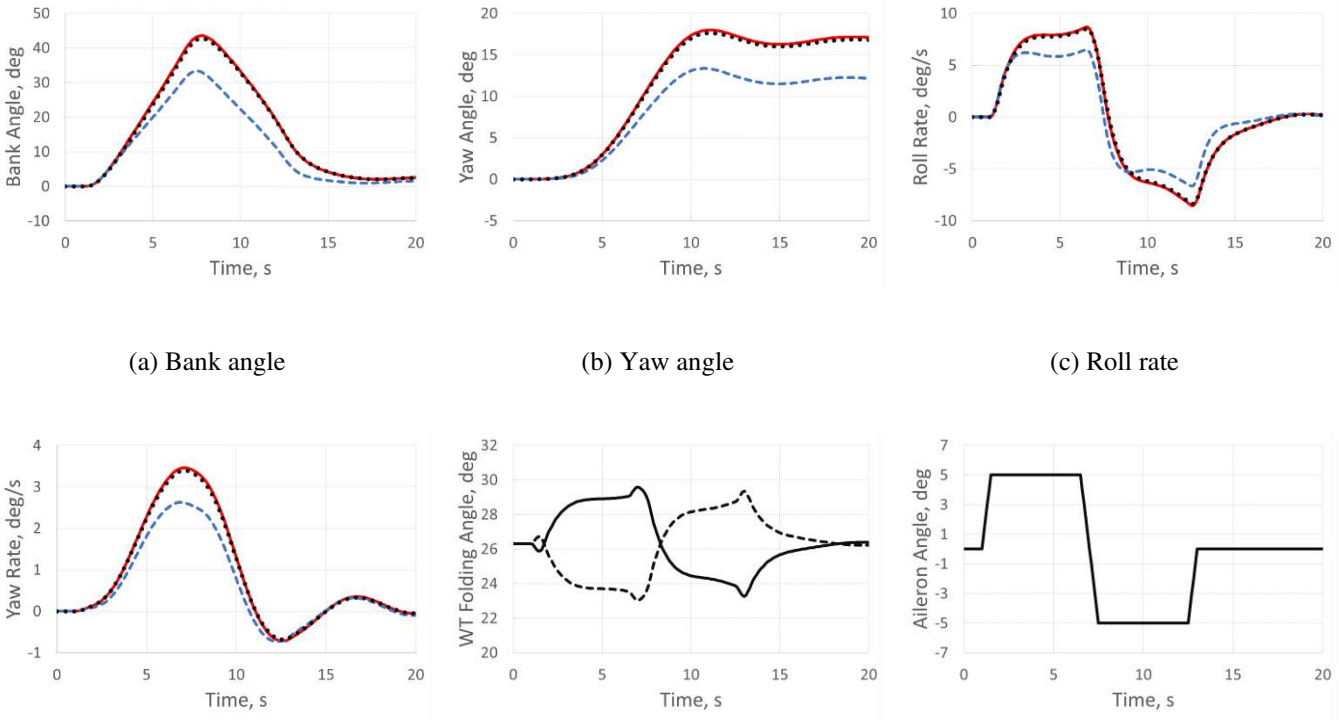

(a) Bank angle (b) Yaw angle (c) Roll rate

(d) Yaw rate (e) Wing-tip folding angle (f) Aileron deflection

Figure 6. Dynamic Response Due to an Aileron Deflection

(black dotted line: baseline; blue dashed line: fixed hinge; red solid line: free hinge)

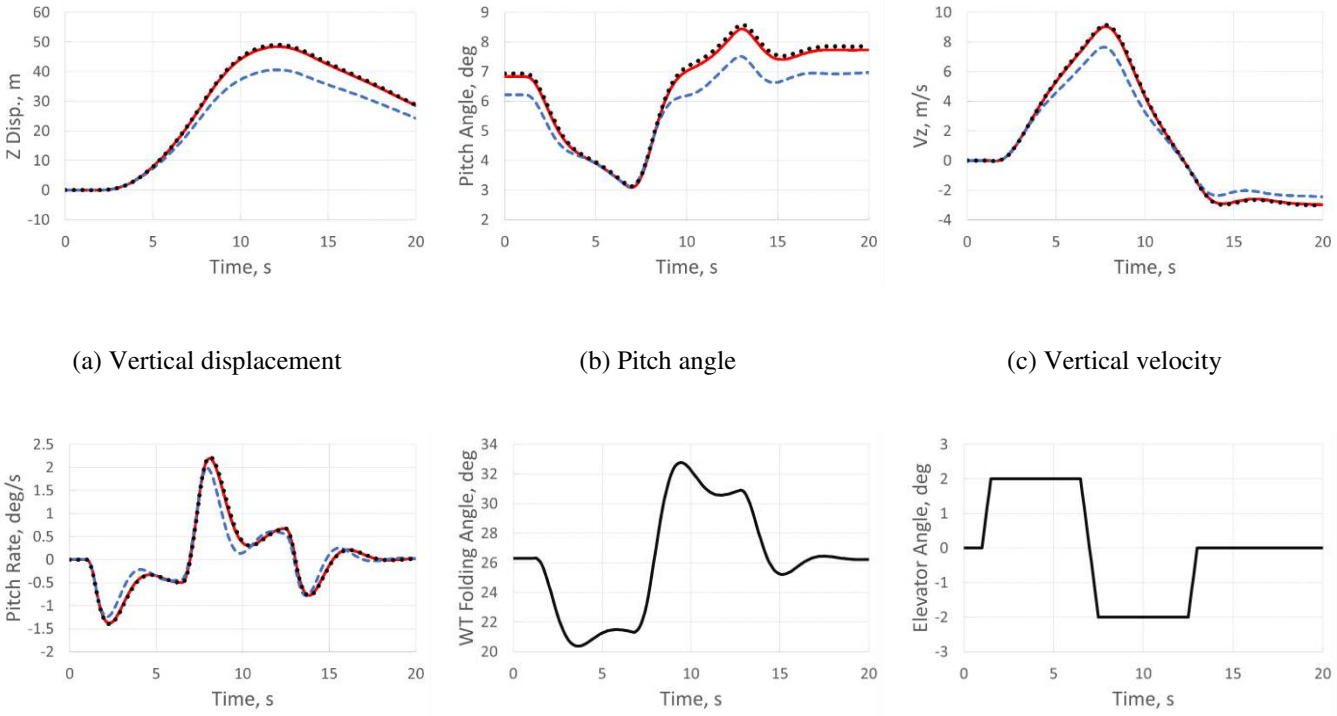

(a) Vertical displacement (b) Pitch angle (c) Vertical velocity

(d) Pitch rate (e) Wing-tip folding angle (f) Elevator deflection

Figure 7. Dynamic Response Due to an Elevator Deflection

(black dotted line: baseline; blue dashed line: fixed hinge; red solid line: free hinge)

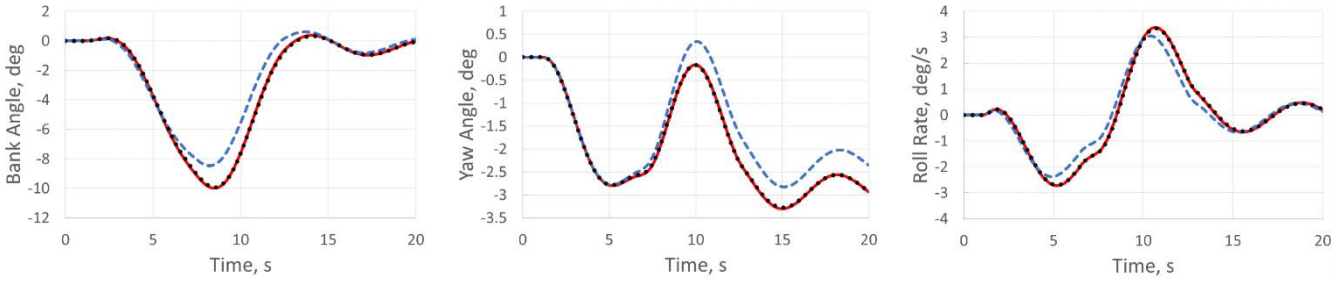

(a) Bank angle (b) Yaw angle (c) Roll rate

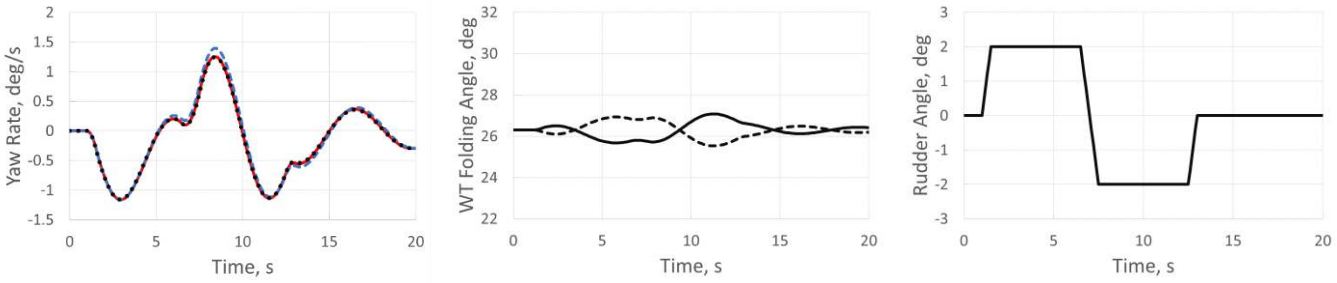

(d) Yaw rate (e) Wing-tip folding angle (f) Rudder deflection

Figure 8. Dynamic Response Due to a Rudder Deflection

(black dotted line: baseline; blue dashed line: fixed hinge; red solid line: free hinge)

C. Gust Response

This section presents the dynamic response of the free flying aircraft due to a "1-cosine" gust. Only one gust length of 214 m is considered and the gust amplitude has been selected according the EASA Regulations [14].

Figure 9 shows the response of the three aircraft in terms of vertical speed and pitch rate induced by the gust. This latter is considered uniform across the wing span. As in the previous case, the free hinge aircraft response is close, if not equal, to the baseline one. The wing-tips act as a dynamic damper reducing the vertical speed and pitch rate experienced by aircraft with respect to the fixed hinge model. Moreover, Fig. 9(b) confirms that the fixed hinge aircraft has a lower short period frequency.

Similar results are reported in Fig(10), but for a non-uniform spanwise gust. In this case the wing-tips damp the perturbation introduced by the gust in terms of roll and yaw rate.

Figure 11 shows the long-term response to a uniform spanwise gust. The same long period response is observed for the three models, confirming as reported in Fig. 5(a).

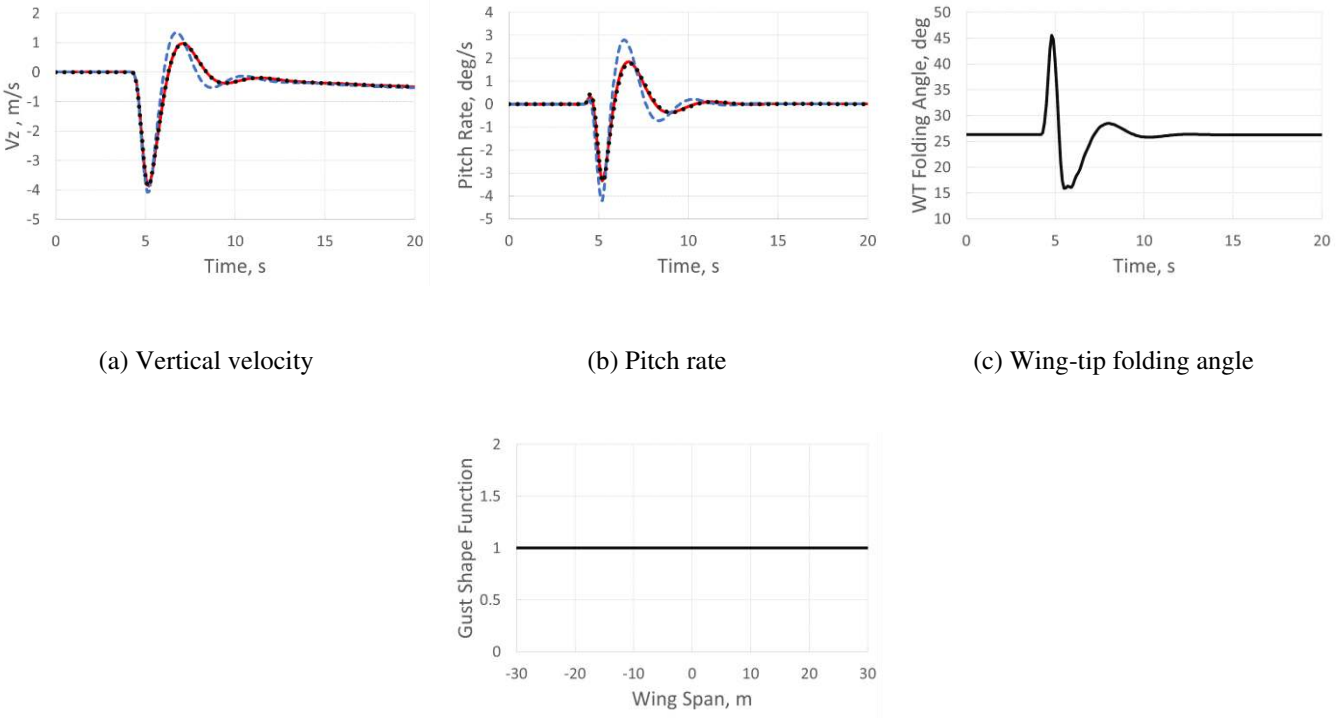

(a) Vertical velocity (b) Pitch rate (c) Wing-tip folding angle

(d) Spanwise gust shape function

Figure 9. Dynamic Gust Response

(black dotted line: baseline; blue dashed line: fixed hinge; red solid line: free hinge)

D. Dynamic wing-tip release

The SAH wing-tip concept is based upon the idea of having the wing-tips fixed during the cruise condition, in order to maximize the aerodynamic benefits due to the longer span, and to release them only when needed, both to reduce the loads or enhance the aircraft manoeuvrability. A question arises as to what would be the dynamic response of the aircraft induced by the wing-tips release. Figure 12 shows some related interesting quantities. As soon as the hinge is released, the wing-tip tend to rotate upward to their free-floating equilibrium position. This leads to the generation of local negative incremental aerodynamic forces at the tips, which reflects also in a pitch up moment. As a consequence, the wing-tips release excites both the short and the long period. However, such excitation results to be lower in magnitude with respect to the perturbation induced by a gust. Moreover, after the wing tip is released a

variation on the elevator angle is also required in order to balance the pitching moment induced by the tip deflection [15].

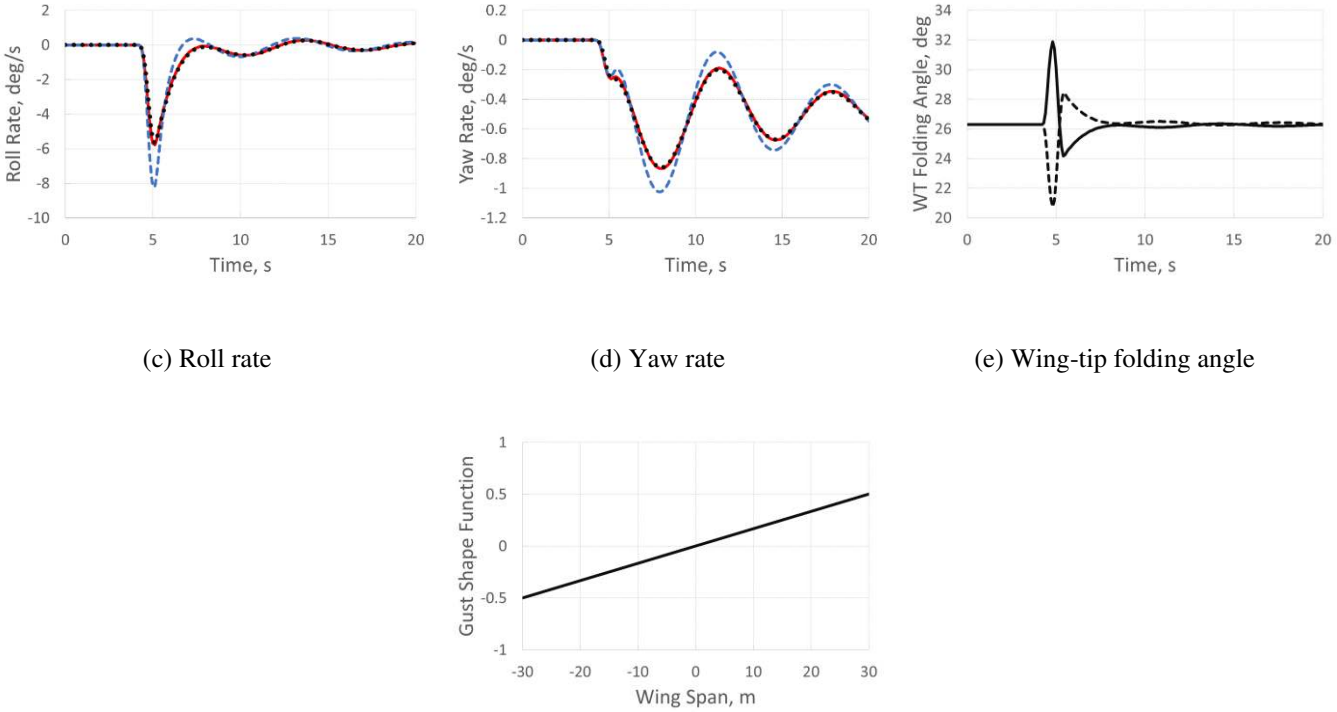

(c) Roll rate (d) Yaw rate (e) Wing-tip folding angle

(f) Spanwise gust shape function

Figure 10. Dynamic Gust Response (asymmetric spanwise distribution)

(black dotted line: baseline; blue dashed line: fixed hinge; red solid line: free hinge)

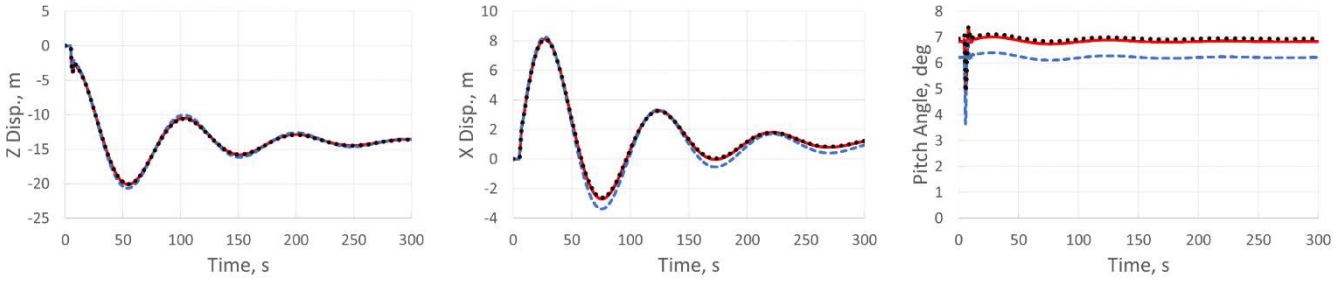

(a) Vertical displacement (b) Longitudinal displacement (c) Pitch rate

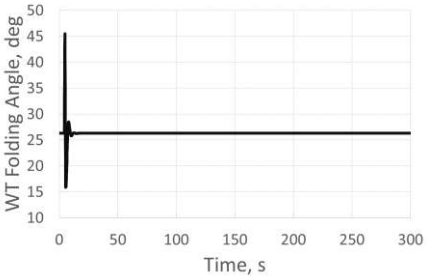

(d) Wing-tip folding angle

Figure 11. Dynamic Gust Response (long term response)

(black dotted line: baseline; blue dashed line: fixed hinge; red solid line: free hinge)

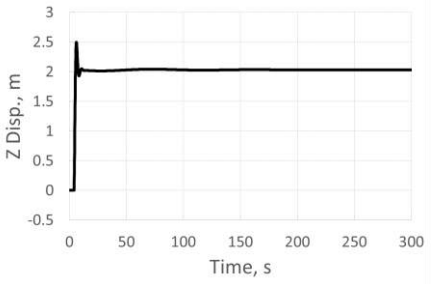

(a) Vertical displacement

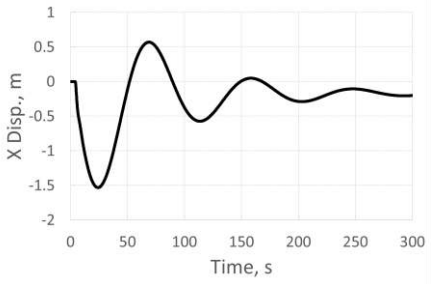

(b) Longitudinal displacement

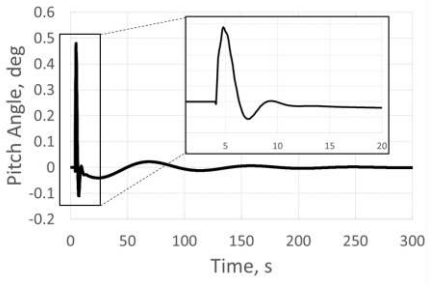

(c) Pitch rate

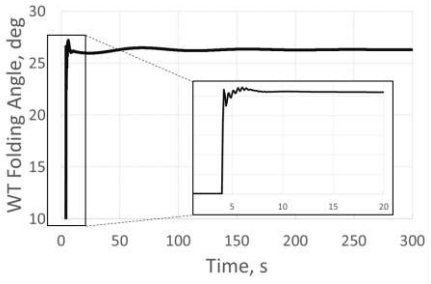

(d) Wing-tip folding angle

Figure 12. Dynamic Wing-Tips Release Response

IV. Conclusions

A preliminary analysis of the impact of the SAH on the aircraft flight dynamics has been investigated. The results have shown that despite the 25% increment in span, the free hinge aircraft has the same handling qualities and dynamic response of the baseline model with no wing-tip extension. Such a finding extends the applicability of the SAH which can be used both as loads reduction device but also to alleviate the roll damping increment induced by the longer span. This results in an enhanced aileron authority with a consequent weight saving, with respect to the fixed hinge aircraft, due to the smaller aileron size required.

A free wing-tip will passively do whatever it takes to satisfy the condition of zero hinge moment condition, this results in the tip attitude to offload itself, thus minimizing his impact on the loads and handling qualities when compared to an aircraft without the wing extension.

Future work will be focused on the introduction of a multibody formulation of the aircraft/wing-tips system in order to investigate the impact of the geometric nonlinear effects due to the wing-tip deflection both on the aircraft loads and flight dynamics.

References

1. A. Castrichini , V. Hodigere Siddaramaiah , D.E. Calderon, J.E. Cooper, T. Wilson, Y. Lemmens Preliminary Investigation of Use of Flexible Folding Wing-Tips for Static and Dynamic Loads Alleviation. Aeronautical Journal Volume 121, Issue 1235 January 2017, pp. 73-94
2. Castrichini A.,Hodigere Siddaramaiah V., Calderon D.E., Cooper J.E.,Wilson T., Lemmens, Y. “Nonlinear Folding Wing Tips for Gust Loads Alleviation, Journal of Aircraft”, published online 17 Feb. 2016. Doi: http://dx.doi.org/10.2514/1.C033474.
3. A Castrichini J E.Cooper, T Wilson, A Carella & Y Lemmens "Nonlinear Negative Stiffness Wing-Tip Spring Device for Gust Loads Alleviation" , Journal of Aircraft, Vol. 54 (2017), pp. 627-641.
4. R.C.M. Cheung, D. Rezgui, J.E. Cooper, and T. Wilson. "Testing of a Hinged Wingtip Device for Gust Loads Alleviation", Journal of Aircraft. https://doi.org/10.2514/1.C034811
5. T. Wilson, A. Azabal, A. Castrichini, J.E. Cooper, R. Ajaj and M. Herring (2016) “Aeroelastic behaviour of

hinged wing tips". International Forum on Aeroelasticity and Structural Dynamics, IFASD 2017.

6. F. Saltari, C. Riso, G. De Matteis, F. Mastroddi, "Finite-Element-Based Modeling for Flight Dynamics and Aeroelasticity of Flexible Aircraft", Journal of Aircraft 2017 54:6, 2350-2366.
7. Canavin, J.R., Likins, P.W., "Floating Reference Frames for Flexible Spacecraft", Journal of Spacecraft and Rockets, 14(12):724–732, December 1977.
8. Meirovitch, L., Tuzcu, I., "The Lure of the Mean Axes", Journal of Applied Mechanics, 74(3), 497-504, 2007.
9. Waszak, M.R., Buttrill, C.S., Schmidt, D.K., Modeling and Model Simplification of Aeroelastic Vehicles: An Overview, NASA Technical Memorandum 107691, 1992.
10. Looye, G., "Integration of rigid and aeroelastic aircraft models using the residualised model method", International Forum on Aeroelasticity and Structural Dynamics, number IF-046. CEAS/DLR/AIAAA, 2005.
11. Kier, T., "Comparison of Unsteady Aerodynamic Modelling Methodologies with Respect to Flight Loads Analysis", AIAA Atmospheric Flight Mechanics Conference and Exhibit, 2005.
12. Albano E., Rodden W.P., "A Doublet-Lattice Method for Calculating Lift Distributions on Oscillating Surfaces in Subsonic Flows", AIAA Journal v7 n2 1969 pp 279-285.
13. Rodden W.P., Johnson E.H. , "MSC/NASTRAN Aeroelastic Analysis' User's Guide", MSC Software, USA, 1994.
14. Certification Specifications for Large Aeroplanes CS-25, EASA, 2007.
15. Roger K.L., "Airplane Math Modeling Methods For Active Control Design", AGARD Structures and Materials Panel, number CP-228, pp 4-11, 1977.
16. A. Castrichini, T. Wilson, J.E. Cooper, "On the Dynamic Release of the Semi Aeroelastic Hinge Wing-Tip Device", RAeS 6th Aerospace Structures Design Conference, 2018